Hydrocephalus, massive myelitis, and adhesive arachnoiditis: full neuroaxis involvement by neurocryptococcosis

Hidrocefalia, mielite maciça e aracnoidite adesiva: envolvimento de todo o neuroeixo por neurocriptococose

André Eduardo de Almeida Franzoi[1] Tamiris Maier Silva Ferreira[2]
Emanuele Therezinha Schueda Stonoga[3] Bernardo Corrêa de Almeida Teixeira[4]
Rosana Herminia Scola[5]

[1] Universidade Federal do Paraná, Hospital de Clínicas, Serviço de Neurologia, Departamento de Clínica Médica, Curitiba PR, Brazil.
[2] Universidade Federal do Paraná, Hospital de Clínicas, Serviço de Infectologia, Departamento de Clínica Médica, Curitiba PR, Brazil.
[3] Universidade Federal do Paraná, Hospital de Clínicas, Serviço de Anatomia Patológica e Histopatologia, Departamento de Clínica Médica, Curitiba PR, Brazil.
[4] Universidade Federal do Paraná, Hospital de Clínicas, Serviço de Radiologia, Departamento de Clínica Médica, Curitiba PR, Brazil.
[5] Universidade Federal do Paraná, Hospital de Clínicas, Serviço de Doenças Neuromusculares, Departamento de Clínica Médica, Curitiba PR, Brazil.

Address for correspondence André Eduardo de Almeida Franzoi (email: andrefranzoi@hotmail.com).

Arq. Neuropsiquiatr. 2023;81:607–609.

A 37-year-old male patient presented with subacute paraparesis, urinary incontinence, and a sensory level of T8. An analysis of the cerebrospinal fluid revealed lymphocytic pleocytosis (5 white blood cells/mm^3), low levels of glucose (25 mg/dL), increased levels of protein (713 mg/dL), high levels of lactic acid (4.7 mmol/L), and positive cryptococcal antigen. A magnetic resonance imaging (MRI) scan showed hydrocephalus (►**Figure 1**), myelopathy (►**Figure 2**), and adhesive arachnoiditis (►**Figure 3**). Meningeal biopsy showed round cells suggestive of cryptococcosis (►**Figure 4**), without species differentiation in the culture samples. *Cryptococcus* may exhibit unique clinical manifestations, such as gelatinous pseudocysts in the basal ganglia, cerebral cryptococcomas, leptomeningitis, cranial neuropathies, adhesive arachnoiditis, and obstructive hydrocephalus.[1–5]

Authors' Contributions

All authors contributed to the conception and design of the study. AEAF: performed material preparation, data collection and analysis, and wrote the first draft of the manuscript, and all authors commented on previous versions and read and approved the final manuscript.

Conflict of Interest

The authors have no conflict of interest to declare.

Acknowledgments

We would like to thank the Neurosurgery Service at Hospital de Clínicas (HC), Universidade Federal do Paraná (UFPR), Curitiba, Brazil), which provided assistance in the meningeal biopsy of the patient.

received
November 22, 2022
received in its final form
February 11, 2023
accepted
February 15, 2023

DOI https://doi.org/10.1055/s-0043-1768159.
ISSN 0004-282X.

Thieme Revinter Publicações Ltda., Rua do Matoso 170, Rio de Janeiro, RJ, CEP 20270-135, Brazil

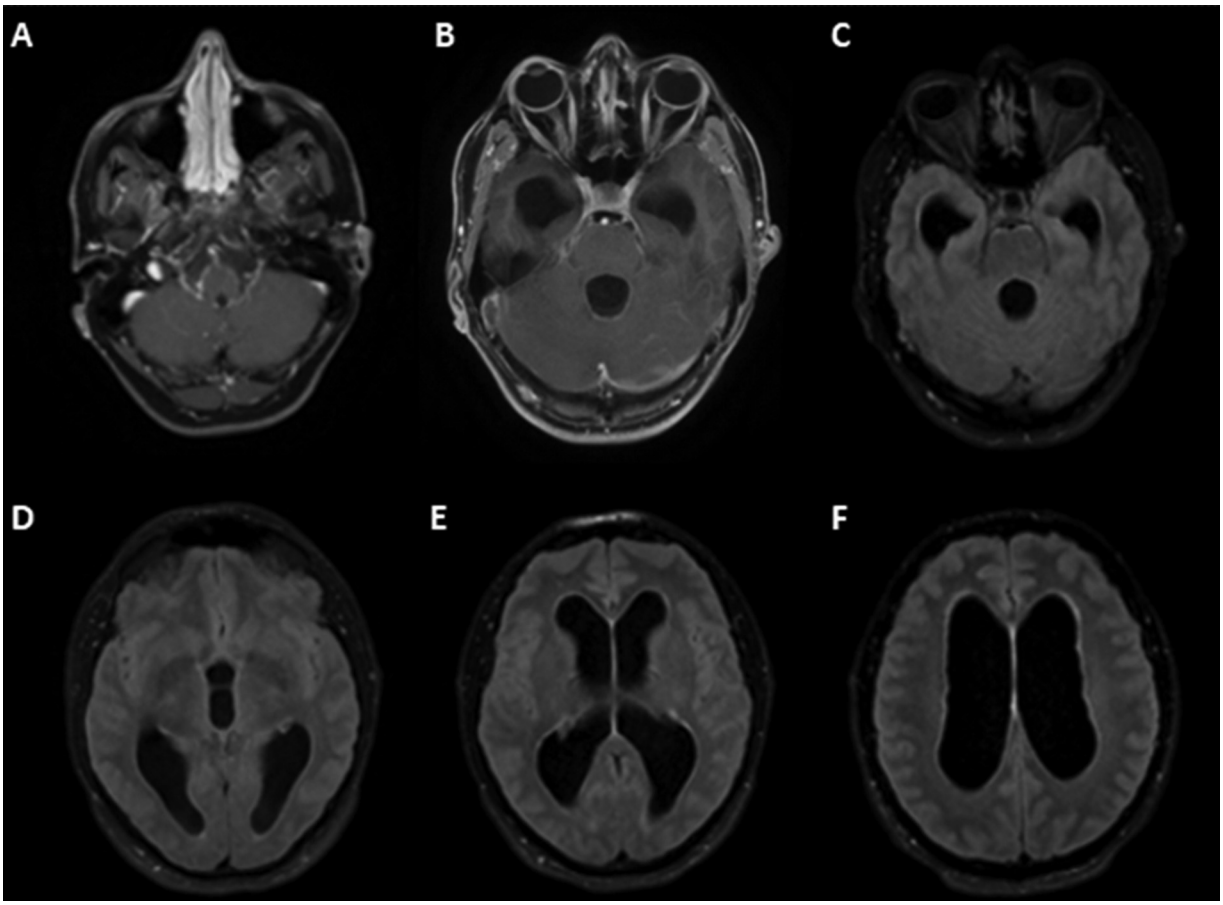

Figure 1 (**A**,**B**) Axial contrast-enhanced T1-weighted magnetic resonance imaging (MRI) scan revealing leptomeningeal enhancement at the base of the brain in the posterior fossa; (**C–F**) axial fluid-attenuated inversion recovery (FLAIR) MRI showing hydrocephalus throughout the ventricular system, without significant transudation of the cerebrospinal fluid.

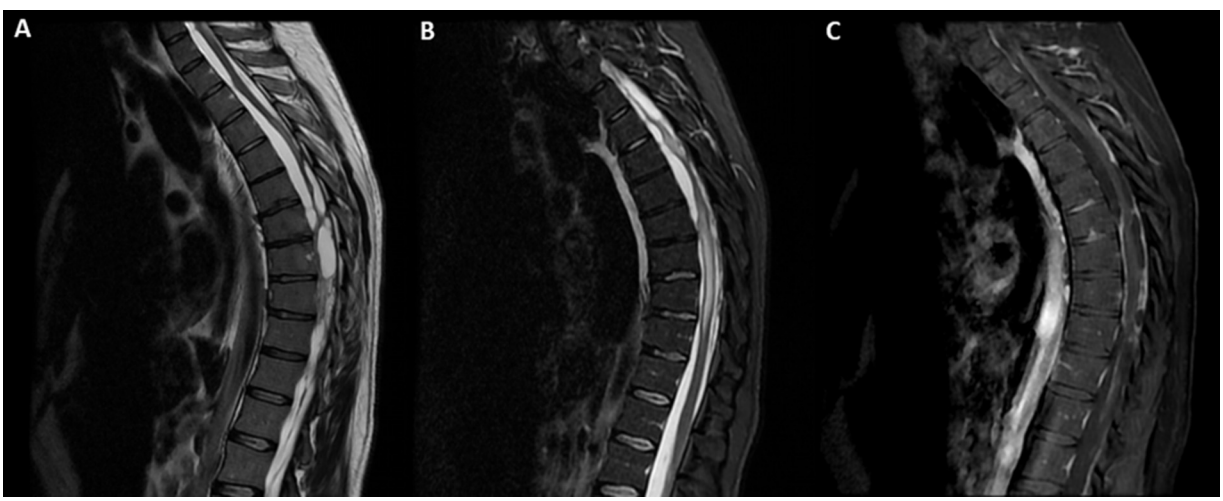

Figure 2 (**A**) Sagittal T2-weighted MRI showing septations in the subarachnoid space around the spinal cord; (**B**) sagittal short-tau inversion recovery (STIR) MRI showing hyperintensity and distortion in the spinal cord; (**C**) sagittal contrast-enhanced T1-weighted MRI revealing leptomeningeal enhancement around the entire spinal canal.

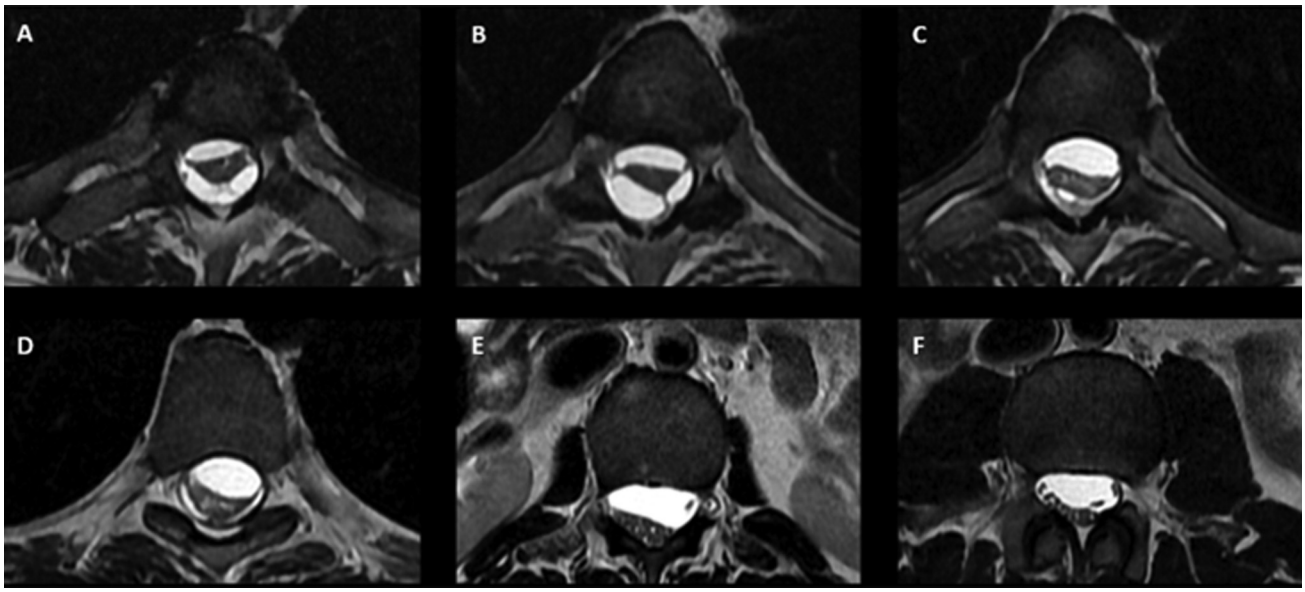

Figure 3 (**A–D**): Axial T2-weighted MRI showing adhesive arachnoiditis and septations distorting the spinal cord at the level of the thoracic spinal cord; (**E,F**) axial T2-weighted MRI showing adhesive arachnoiditis and septations distorting the spinal cord at the level of the lumbosacral spinal cord.

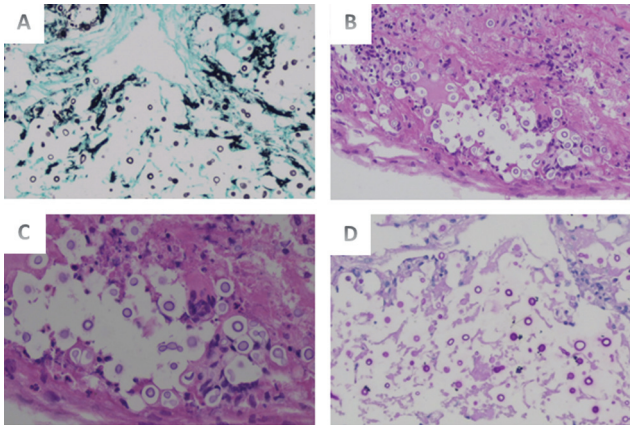

Figure 4 Encapsulated, spherical-to-oval yeast cells (5–10 µm in diameter) with narrow-based budding and polysaccharide capsules. The yeast cells vary in size, and the organisms can be capsule-deficient. (**A**) Grocott methenamine silver (GMS), smallest increase (×20); yeast cells tested positive for GMS; (**B**) hematoxylin and eosin staining, the smallest increase (×20); (**C**) periodic acid Schiff–diastase (PAS–D), highest magnification (×40); yeast cells tested positive for PAS–D staining; (**D**) PAS–D, smallest increase (×20).

References

1 Maziarz EK, Perfect JR. Cryptococcosis. Infect Dis Clin North Am 2016;30(01):179–206. Doi: 10.1016/j.idc.2015.10.006
2 Eshwara VK, Garg R, Chandrashekhar GS, Shaw T, Mukhopadhyay C. Fatal *Cryptococcus gattii* meningitis with negative cryptococcal antigen test in a HIV-non-infected patient. Indian J Med Microbiol 2018;36(03):439–440. Doi: 10.4103/ijmm.IJMM_18_164
3 Grosse P, Tintelnot K, Söllner O, Schmitz B. Encephalomyelitis due to Cryptococcus neoformans var gattii presenting as spinal tumour: case report and review of the literature. J Neurol Neurosurg Psychiatry 2001;70(01):113–116. Doi: 10.1136/jnnp.70.1.113
4 Agrawal A, Agrawal A, Agrawal C, Rohtagi A. An unusual spinal arachnoiditis. Clin Neurol Neurosurg 2006;108(08):775–779. Doi: 10.1016/j.clineuro.2005.09.007
5 Panackal AA, Komori M, Kosa P, et al. Spinal arachnoiditis as a complication of cryptococcal meningoencephalitis in non-HIV previously healthy adults. Clin Infect Dis 2017;64(03):275–283. Doi: 10.1093/cid/ciw739